[21] Modi, V. J. and Wiland, E., "Unsteady Aerodynamics of Stationary Elliptic Cylinders in Subcritical Flow," *AIAA Journal*, Vol. 8, Oct. 1970, pp. 1814–1821.

[22] Bryer, D. W., Walshe, D. E., and Garner, H. C., "Pressure Probes Selected for Three-Dimensional Flow Measurement," R. and M. No. 3037, 1958, Aeronautical Research Council, London.

[23] Frimberger, R., "Experimentelle Untersuchungen an Kármánschen Wirbelstrassen," *Zeitschrift Flugwiss*, Vol. 5, 1957, pp. 355–359.

[24] Fage, A. and Johansen, F. C., "On the Flow of Air Behind an Inclined Flat Plate of Infinite Span," *Proceedings of the Royal Society of London*, Ser. A, Vol. 116, 1927, pp. 170–197.

[25] Rosenhead, L. and Schwabe, M., "An Experimental Investigation of the Flow Behind Circular Cylinders in Channels of Different Breadths," *Proceedings of the Royal Society of London*, Ser. A, Vol. 129, 1930, pp. 115–135.

[26] Wille, R. and Timme, A., "Über des Verhalten von Wirbelstrassen," *Jahrbuch der Schiffbautechnik Gesellschaft*, Vol. 51, 1957, pp. 215–221.

[27] Tyler, E., "Vortex Formation Behind Obstacles of Various Sections," *The Philosophical Magazine*, Ser. 7, Vol 11, No. 72, 1931, pp. 849–890.

[28] Modi, V. J. and El-Sherbiny, S., "On the Wall Confinement Effects in the Industrial Aerodynamics," Paper 116, *Proceedings of the International Symposium on Vibration Problems in Industry*, U.K. Atomic Energy Authority and National Physical Lab., Keswick, England, 1973.

APRIL 1975 AIAA JOURNAL VOL. 13, NO. 4

Unsteady Aerodynamics of Vehicles in Tubes

ANDREW G. HAMMITT*
Andrew G. Hammitt Associates, Palos Verdes Peninsula, Calif.

The aerodynamics of vehicles traveling through tubes are significantly affected by the constraints of the tube wall and the relative size (blockage ratio) of the vehicle. Steady flow conditions are reached only after long travel times. In this report, the flow created by vehicle travel in a tube is analyzed using numerical integration of the unsteady flow equations. Steady state conditions are rarely obtained for closed-end tubes up to several hundred miles in length. Solutions are presented for various blockage ratio vehicles with choked and unchoked flow conditions about them. Various tube lengths are also considered. The solution for a doubly infinite tube is found to be approaching the asymptotic long time solution.

Nomenclature

A = cross section area of tube
A_{vw} = vehicle surface area
A_{ww} = tube surface area
C_D = drag coefficient of vehicle based on tube area and relative velocity
C_F = skin-friction coefficient
C_p = specific heat, at constant pressure
C = speed of sound
C_{MT} = momentum loss coefficient of vehicle based on tube area and relative velocity
C_H = Stanton number
d = tube diameter
D = drag of vehicle
L = length of vehicle
m = mass flux
M_∞ = $u_s/(\gamma RT_w)^{1/2}$ vehicle Mach number
p = pressure
p^* = p/p_∞
q_r = heat flux to vehicle
q_w = heat flux to wall
R = gas constant
Re_d = Reynolds number based on tube diameter and vehicle velocity
s = entropy
t = time
T = temperature
T^* = T/T_w
T_o = stagnation temperature of air
T_w = temperature of wall
T_{ow} = stagnation temperature of wall
T_{aw} = adiabatic wall temperature
u = velocity of air relative to tube
u^* = u/u_s
u_s = velocity of vehicle relative to tube
v = velocity of air relative to vehicle, $v = u - u_s$
v^* = v/u_s
x = distance along tube
β = vehicle area blockage ratio, area of vehicle/area of tube
γ = specific heat ratio
λ = $2C_f L/(1-\beta)$
ρ = fluid density
τ_w = wall shear stress
τ_v = vehicle surface shear stress

Received March 7, 1974; revision received October 15, 1974. This work was sponsored by Office of Research, Development and Demonstrations, Federal Railroad Administration, U.S. Department of Transportation.

Index categories: Nonsteady Aerodynamics; Nozzle and Channel Flow.

* President. Member AIAA.

Introduction

THE interest in high-speed ground transportation has lead to a variety of suggested systems. Because the aerodynamic drag of a ground vehicle when operating at high speed in the open is quite large, it has been suggested that vehicles be placed in evacuated or semi-evacuated tubes. A necessary step in the development of such systems is an understanding of the applicable aerodynamics. The presence of the tube has two important effects: 1) it restricts the free passage of air about the vehicle, and 2) it confines the disturbances which originate at the vehicle from dissipating in three dimensions. Tube vehicle systems can be classified in many ways. For aerodynamic purposes, the most important parameters are the speed and blockage ratio of the vehicle, the tube length, and the means of propulsion. The importance of speed and blockage are obvious. If the tube is sufficiently long or the time of travel of the vehicle is sufficiently short, then the vehicle behavior will not be influenced by the tube ends. The type of propulsion system which is used has an important influence on the system design and

the system aerodynamics. Vehicles drawn by force from the tube wall are the type considered in this study and will be called externally propelled. It is convenient to consider the flowfield divided into two regions: 1) a far flowfield which covers the whole length of the tube excluding the region of the vehicle, and several tube diameters in front of and behind the vehicle; and 2) a near flowfield which covers this excluded region. The advantage of this division is that the far flowfield can be treated as a one-dimensional unsteady flow and the near flowfield as a steady flowfield in vehicle-fixed coordinates and several space dimensions. For large L/d ratio vehicles, it will be found that a quasi-one-dimensional approach is adequate for the near flowfield.

The confinement of the tube walls has important effects upon the near flowfield. If the flow sufficiently far ahead of and behind the vehicle is considered, then the confining tube walls required that the mass flux (in vehicle-fixed coordinates) both ahead of and behind the vehicles are equal. The velocity or momentum flux relative to the vehicle must be the same, if the flow is incompressible; or increased behind the body, if the flow is compressible. A pressure drop across the vehicle is required to provide the drag force on the vehicle. This situation is identical to steady pipe flow where the drag of the walls causes the pressure to drop and, in the compressible case, the flow to accelerate.

The flow will be accelerated through the narrow annular passages about the vehicle with the result that it will reach Mach 1 for moderate flow Mach number ahead of the vehicle. The Mach number ahead of the vehicle, when choking in the annular passage occurs, is the maximum Mach number possible in front of the vehicle. When the flow about the vehicle is choked, then the flow conditions behind the vehicle can no longer influence those in front of the vehicle. The vehicle drag is no longer directly related to the vehicle characteristics, but more closely associated with the tube characteristics. In expanding from the sonic section, the flow may either accelerate to supersonic velocities and be shocked back to subsonic or diffuse smoothly to subsonic velocity. The process that actually occurs depends upon the downstream conditions just as in a convergent-divergent nozzle.

The near flowfield is coupled to the far flowfield. For the unchoked case, a pressure drop related to the vehicle drag provides the matching condition. For the choked case, matching of the relative Mach number is required. The far flowfield, when coupled to the near flowfield, determines the relative Mach number ahead of the vehicle for the unchoked case. For the choked case, the far flowfield determines the pressure ahead of and behind the vehicle, and the drag.

The far flowfield is caused by the vehicle starting transient. This transient causes pressure waves that propagate for long distances down the tube. The tube confines these waves so they cannot dissipate in three dimensions but are attenuated by heat transfer and friction with the tube walls. The far flowfield is essentially unsteady, but two simplified steady solutions (in correctly selected coordinate systems) can be obtained in both the limit of short and long time after the initiation of the vehicle motion. Soon after the vehicle has started, heat transfer and friction have not had time to affect the far flowfield, and the waves have only traveled a relatively short distance down the tube. The relatively weak waves caused by a vehicle moving with subsonic velocity are essentially isentropic. The flow across such waves can be described by one-dimensional steady relations, if a coordinate system moving with the waves is adopted. In the limit of very long times, the waves are completely dissipated by friction and heat transfer, and the far flowfield becomes steady in a vehicle-fixed coordinate system. The pressure gradients in the tube are balanced by the friction on the tube walls. While these two steady solutions are available for short and long times[1-2] the intermediate time solutions are not steady in any coordinate system, and a solution to a one-dimensional unsteady flow problem with friction and heat transfer is required. These relations must be solved by numerical methods. The purpose of this study is to provide such numerical solutions.

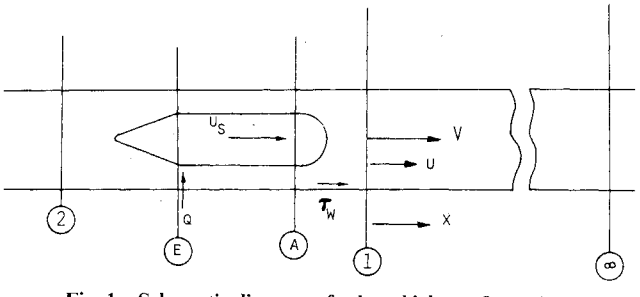

Fig. 1 Schematic diagram of tube vehicle configuration.

The far flowfield is the mechanism which alleviates the need for all the fluid to flow through the annulus about the body. The body may push fluid ahead of it down the tube. If the body has low drag and blockage, then little fluid is pushed down the tube, and the fluid flows about the vehicle. If the flow is choked about the vehicle, a very severe limitation is imposed upon the rate of flow past the vehicle and fluid must be pushed ahead of it. There is no limit on maximum vehicle speed caused by the choking phenomena. The fluid is pushed ahead of the vehicle, as required, to cause any required Mach number relative to the vehicle.

The actual tube vehicle problem involves a vehicle in a tube traveling between two stations near the ends of the tube with intermediate stops. The presence of and location of the ends of the tube, the acceleration and deceleration rate of the vehicle, and the location and duration of the intermediate stops all have an influence on the aerodynamics of the flow and the drag of the vehicle.

It is the purpose of this study to assess the magnitude and the importance of these effects. This assessment will be accomplished by considering two different vehicle configurations, one which results in choked flow at the speeds considered and one which does not. Three tube-end configurations are also considered: ends infinitely far from the vehicle in both directions, a closed end not far behind the vehicle's starting point, and a closed end not far ahead of the vehicle's stopping point. These cases should give an initial assessment of the effect of closed tube ends on the conditions in the tube.

Near Flowfield

The near flowfield describes the flow about the vehicle and extends over that distance in front of and behind the body in which the two-dimensional nature or the change in cross-sectional area of the flow must be taken into account. In most cases it can be considered to be steady flow with time varying boundary conditions. The flowfield is best considered in vehicle fixed coordinates as shown in Fig. 1. The flow, relative to the vehicle, accelerates into the annular space between the vehicle and the tube. This flow is essentially isentropic and involves an increase in velocity and Mach number. The area ratio and relative Mach number ahead of the vehicle are limited to values that give a Mach number in the annular passage less than one. As the fluid flows throughout the annular passage, friction with the vehicle and the tube wall and heat transfer with the tube wall are all important effects. There can be no heat transfer with the vehicle unless the vehicle contains an energy source or sink. An energy source is quite possible for some configurations but will not be considered in this analysis. The combined effect of this heat transfer and friction is to increase the Mach number. A Mach number equal to one is the maximum value that can be reached at the exit from the annular passage. The flow then passes over the rear of the vehicle and eventually fills the entire tube behind the vehicle. In the ideal situation this flow over the back of the vehicle could be isentropic. This condition can be approached if a vehicle with a long pointed tail is used. If a blunt based vehicle is used, the flow will separate at the base. Under this

condition the usual assumption, at least for low-speed conditions, is that the base pressure is equal to the static pressure in the annulus at the base. Lower base pressures might be expected at higher vehicle Mach numbers.

If the compressible flow equations are written in a coordinate system fixed with the vehicle, the results are as follows:

Continuity

$$\frac{1}{\rho}\frac{\partial \rho}{\partial x}+\frac{1}{v}\frac{dv}{dx}+\frac{1}{A}\frac{dA}{dx}=0 \tag{1}$$

Momentum

$$\frac{dp}{dx}+\tau_w\frac{1}{A}\frac{dA_{ww}}{dx}+\tau_v\frac{1}{A}\frac{dA_{vw}}{dx}+\rho v\frac{dv}{dx}=0 \tag{2}$$

Energy

$$\left(C_p\frac{dT}{dx}+\frac{d(v^2/2)}{dx}\right)\rho v=(\tau_w u_s+q_w)\frac{1}{A}\frac{dA_{ww}}{dx}+\frac{q_v}{A}\frac{dA_{vw}}{dx} \tag{3}$$

State

$$p=\rho RT \tag{4}$$

A_{ww} and A_{vw} are the tube and vehicle wall surface area and A is the flow cross-sectional area. The assumption will be made that there is no heat transfer to the vehicle, $q_v=0$. This condition would have to be modified for a vehicle that dissipated power directly as heat. The friction force on the vehicle does not enter the energy Eq. (3), since this friction force is acting on a surface that is stationary with respect to the coordinate system and therefore does no work. The friction force and heat transfer can both be expressed in coefficient form by the relations

$$\tau_w=\tfrac{1}{2}\rho u|u|C_f \tag{5}$$

$$\tau_v=\tfrac{1}{2}\rho v|v|C_f \tag{6}$$

$$q_w=\rho|u|C_p(T_w-T_{aw})C_H \tag{7}$$

where

$$T_{aw}=T+(u^2/2C_p) \tag{8}$$

The heat transfer coefficient is related to the friction coefficient by Reynold's analogy.

$$C_H=\tfrac{1}{2}C_f \tag{9}$$

For circular vehicle and tube the relations for A_{ww} and A_{vw} are

$$\frac{1}{A}\frac{dA_{ww}}{dx}=\frac{4}{d(1-\beta)} \tag{10}$$

$$\frac{1}{A}\frac{dA_{vw}}{dx}=\frac{4\beta^{1/2}}{d(1-\beta)} \tag{11}$$

The energy Eq. (3) can now be written in the form

$$\rho v\frac{dT_o}{dx}=\frac{2C_f\rho|u|}{d(1-\beta)}(T_{ow}-T_o) \tag{12}$$

where

$$T_o=T+(v^2/2C_p)$$

and

$$T_{ow}=T_w+(u_s^2/2C_p)$$

A simple solution to this equation is $T_o=T_{ow}$ which is a constant. This solution is the correct one if the initial conditions in front of the vehicle are such that the stagnation temperature of the air is the value it would have if it were at wall temperature and moving at wall velocity.

The fluid incurs a momentum loss in flowing about the vehicle which is caused by the drag exerted on the vehicle and on the tube wall. The friction force on the tube wall affects the vehicle drag by causing an increase in the pressure drop along the annular passage. This increased pressure drop causes a lower pressure on the base of the vehicle and consequently an increase in the drag of the vehicle. The direct friction force on the tube wall does not affect the vehicle drag except as it acts through the pressure effect. The momentum loss of the fluid in flowing around the vehicle is affected by both the force that the vehicle exerts on the fluid, its drag, and the force that the wall exerts on the fluid. The momentum loss of the fluid and the drag on the vehicle differ by the amount of the friction force on the tube wall.

The possibility of a loss at the nose of the body has been considered in several of the experimental studies of near flowfield tube vehicle aerodynamics. In the studies performed by Gouse et al at MIT and Carnegie-Mellon Institute,[3] the presence of a loss in stagnation pressure at the nose was not measured or considered. In the later work at GASL,[4] a nose loss coefficient was interpreted from the measured pressure distributions. This same approach was used in the experiments run at JPL.[5] In the JPL results, the nose loss was sometimes found to be a gain. Under this condition it was not considered to represent a change in stagnation pressure but a departure from the one-dimensional flow assumption that was used in reducing the data. However, experience with orifices has shown that with a small amount of rounding of the inlet, separation can be avoided and an essentially loss free entrance accomplished. The available experimental data for tube vehicles does not appear to justify a change in this result especially since there does not seem to be any plausible reason for such a change.

A base pressure equal to the pressure in the annulus at the base of the vehicle seems to have been the assumption used in reducing all of the experimental studies referenced. The experimental studies, however, do not appear to be good enough to confirm the validity of this assumption. This assumption is the one which is classically used in low speed incompressible flow and is used in deriving the Borda-Carnot loss for a sudden expansion. This same condition appears to be valid for all subsonic annulus exit speeds. When sonic velocity is reached at the exit of the annulus, the flow can expand supersonically into the base region resulting in a reduced base pressure. This is the mechanism that can lead to the increase in drag coefficient that takes place for the choked flow condition. As has been discussed previously, the base flow is then determined by the conditions set by the far flowfield and cannot be determined by near flowfield considerations.

If the flow quantities are nondimensionalized by the ambient conditions in the tube, Eqs. (1) through (12) can be combined, in the annular passage of constant cross-sectional area about the vehicle, to give

$$\frac{v^*}{p^*}\frac{dp^*}{dv^*}=\frac{\left(\dfrac{u|u^*|+v|v^*|\beta^{1/2}}{v^{*2}}\right)\left[1+(\gamma-1)\dfrac{v^{*2}}{T^*}M_\infty^{\,2}\right]+\dfrac{|u^*|}{v^*}\dfrac{T_w^*-T_{aw}^*}{T^*}}{\dfrac{|u^*|}{v^*}\left(\dfrac{T_w^*-T_{aw}^*}{T^*}\right)\dfrac{T^*}{v^*}\dfrac{1}{\gamma M_\infty^{\,2}}+\dfrac{u|u^*|+v|v^*|\beta^{1/2}}{v^{*2}}} \tag{13}$$

$$\frac{1}{v^*}\frac{(1-\beta)}{2C_f}\frac{dv^*}{dx}=\frac{\dfrac{|u^*|}{v}\left(\dfrac{T_w^*-T_{aw}^*}{T^*}\right)\dfrac{T^*}{v^{*2}}\dfrac{1}{M_\infty^{\,2}}+\gamma\dfrac{u^*|u^*|+v^*|v^*|\beta^{1/2}}{v^{*2}}}{\dfrac{T^*}{v^{*2}}\dfrac{1}{M_\infty^{\,2}}-1} \tag{14}$$

where

$$T^*+\frac{\gamma-1}{2}v^{*2}M_\infty^{\,2}=T_{ow}^*$$

from the solution given to Eq. (12). The conditions at the entrance to the annulus can now be found for any particular set of conditions just ahead of the vehicle by the isentropic flow relations between these two points. These conditions are then used as the initial conditions from which to integrate Eqs. (13) and (14). The momentum loss coefficient can then be calculated by the relation

$$C_{MT}=\frac{1+\gamma M_1^{\,2}-(p_e/p_1)[(1+\gamma M_e^{\,2})(1-\beta)+\beta]}{(\gamma/2)M_1^{\,2}} \tag{15}$$

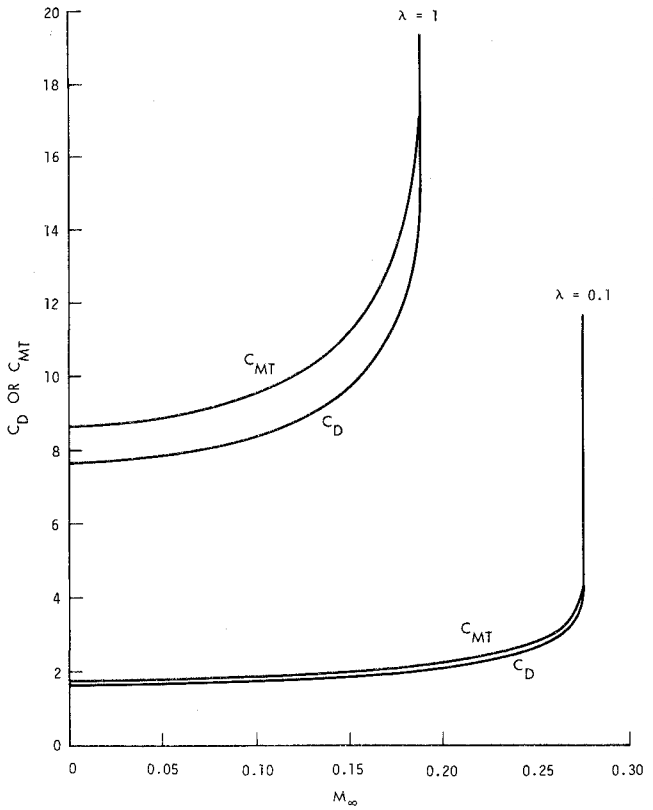

Fig. 2 Near flowfield drag and momentum coefficients, $\beta = 0.5$.

Calculations for the momentum loss and drag coefficients for vehicles of several blockage ratios and lengths are shown in Figs. 2 and 3. These cases are all for conditions of zero fluid velocity and equilibrium temperature. For all these cases, the momentum loss coefficient is slightly larger than the drag coefficient. The character of the two curves is similar. As the Mach number increases from zero, they are relatively flat until the Mach number reaches an appreciable part of the choking Mach number. At that point, the momentum loss or drag coefficient starts to rise relatively rapidly and becomes vertical when it reaches the choking Mach number. At the choking Mach number, the coefficients can have any value above the minimum specified by these curves. However, the drag coefficient must always be less than the momentum loss coefficient by the same amount as at the choking Mach number.

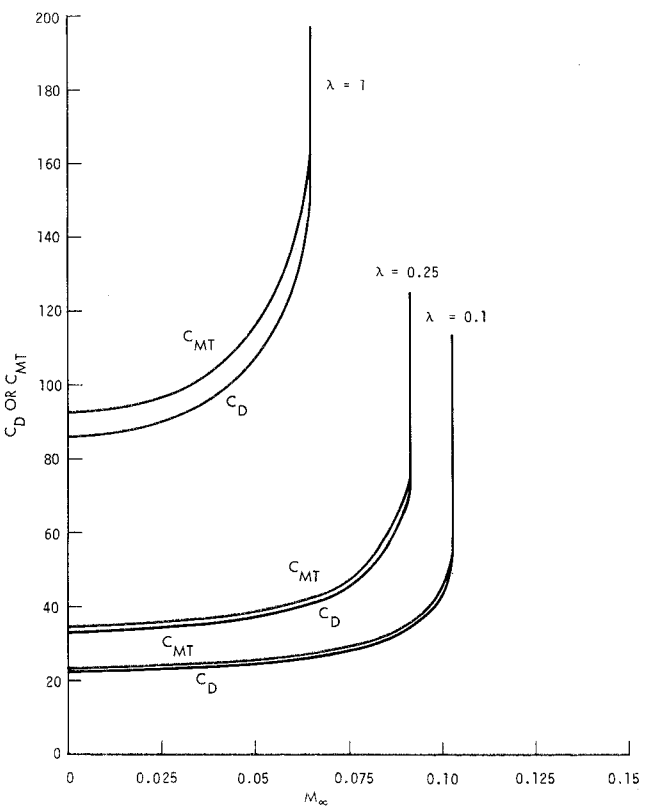

Fig. 3 Near flowfield drag and momentum loss coefficients, $\beta = 0.8$.

The effect of changes in temperature and induced fluid velocity on the drag and momentum loss coefficient have been evaluated. For short vehicles, the effect is small, but it increases with increased vehicle length. The variation in the momentum loss coefficient and drag coefficient with changes in induced flow velocity and temperature was not considered further in this study since these effects do not change the character of the results. These effects can easily be included and should be considered for long vehicles where they would be of greater importance.

Far Flowfield

The far flowfield is that part of the flowfield which lies sufficiently far from the vehicle that it may be considered one dimensional. In the far flowfield the unsteady effects must be taken into account, but by considering regions away from the immediate vicinity of the body, two dimensional or area change effects may be neglected. The solution required is for one space dimensional unsteady flow including friction and heat transfer. This solution involves the integration of a partial differential equation in x and t and must be accomplished by numerical means.

The equations that describe the far flowfield are those of one dimensional unsteady compressible flow. The equations can be written as follows:[6]

Continuity

$$\frac{\partial \rho}{\partial t} + \rho \frac{\partial u}{\partial x} + u \frac{\partial \rho}{\partial x} = 0 \tag{16}$$

Momentum

$$\frac{\partial u}{\partial t} + u \frac{\partial u}{\partial x} + \frac{1}{\rho} \frac{\partial p}{\partial x} + \frac{4\tau_w}{\rho d} = 0 \tag{17}$$

Energy

$$\frac{\partial \rho}{\partial t} + u \frac{\partial p}{\partial x} - C^2 \left(\frac{\partial \rho}{\partial t} + u \frac{\partial \rho}{\partial x} \right) = (\gamma - 1) \frac{4}{d} (q_w + 4\tau_w) \tag{18}$$

These equations have the property that, along special directions in the x,t plane called characteristic direction, they can be written in the form of total differential equations and integrations of these total differential equations carried out along these directions. There are three characteristic directions. The first two directions are given by

$$dx/dt = u \pm C \tag{19}$$

And the third direction by

$$dx/dt = u \tag{20}$$

The first two directions are those taken by disturbances that travel with the speed of sound to either left or right. The third characteristic direction is that of a particle path. Pressure waves follow the characteristics which move with the speed of sound while entropy effects follow the particle paths. The equations that determine the changes in fluid properties along these characteristic directions are as follows:

$$du = \mp \frac{2}{\gamma - 1} dC + \left[\pm \frac{4\gamma q_w}{\rho d C} - \frac{4\tau_w}{\rho d} \left(1 \mp \frac{u}{C} \right) + \frac{C^2}{\gamma} \frac{\partial}{\partial x} \left(\frac{s}{R} \right) \right] dt \tag{21}$$

along the first two characteristics and

$$(ds)_{\text{path}} = (4/\rho\, dT)(u\tau_w + q_w)(dt)_{\text{path}} \tag{22}$$

along the third characteristic.

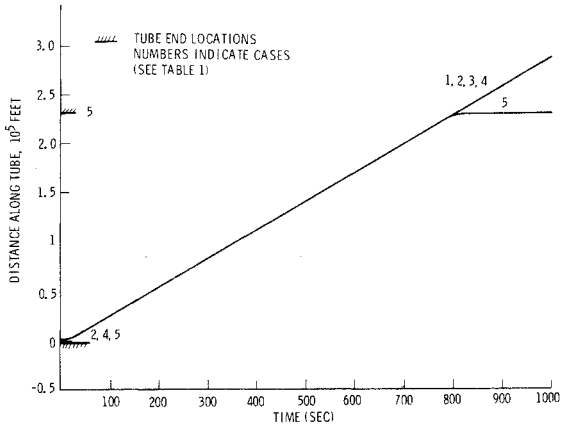

Fig. 4 Vehicle travel as a function of time for the various cases calculated.

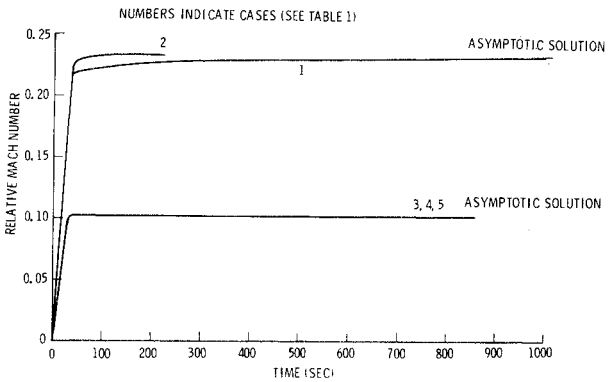

Fig. 5 Relative Mach number as a function of time for Cases 1–5.

These equations can be solved by calculating the direction of the characteristics and the changes that take place along the characteristics. Since the direction of the characteristics depend upon the fluid flow conditions and the changes along the characteristics depend upon the locations of the characteristic mesh points, these solutions are mutually dependent and must be carried out in an iterative fashion.

In the present analysis the assumption is made that the local heat transfer and skin friction depend only on the mean flow properties in the tube and that they are independent of the time rate of change of these properties. This assumption appears to be justified for the rate of change of properties experienced in this problem.[7] However, there is really not yet enough data on the effects of unsteady flow on heat transfer and friction to properly assess this assumption. The friction coefficient is determined by first calculating the Reynolds number and then determining the skin friction coefficient by the relation

$$C_f = 16/Re_d \qquad Re_d < 2500 \tag{23}$$

for a laminar flow condition and

$$4\log_{10}[2Re_d C_f^{1/2}] - 1.6 = C_f^{-1/2} \qquad Re_d > 2500 \tag{24}$$

for a turbulent flow condition. The heat transfer coefficient is then determined by Reynolds analogy, Eq. (9).

An appropriate set of boundary conditions must be placed on the far flowfield which are compatible with the near flowfield solution for flow about the vehicle. For purposes of the far flowfield solution the only input needed from the near flowfield solution is the momentum loss as a function of the relative Mach number (and other appropriate flowfield conditions) and the choking Mach number. An analytical relation is fitted to the momentum loss coefficient Mach number curve to describe this information to the far flowfield solution. If the flow is considered to be adiabatic and steady about the body, the equations that relate the fluid properties behind the vehicle to those in front are as follows:

Continuity

$$(p_2/C_2^2)(u_2 - u_s) = (p_1/C_1^2)(u_1 - u_s) \tag{25}$$

Energy

$$\frac{C_2^2}{\gamma - 1} + \frac{(u_2 - u_s)^2}{2} = \frac{C_1^2}{\gamma - 1} + \frac{(u_1 - u_s)^2}{2} \tag{26}$$

Momentum

$$p_1 - p_2 + \frac{\gamma p_1}{C_1^2}(u_1 - u_s)^2 - \frac{\gamma p_2}{C_2^2}(u_2 - u_s)^2 = \frac{\gamma}{2}\frac{p_1}{C_1^2}(u_1 - u_s)^2 C_{MT} \tag{27}$$

The point at the front of the vehicle must also lie on a left running far flowfield characteristic and that at the back of the vehicle on a right running characteristic. The relations along these characteristics are given by Eq. (21). This set of equations together with the relation between momentum loss coefficient and Mach number obtained from the near flowfield solution form a complete set for determining the properties about the vehicle. The equations do not allow an explicit solution so an iterative method has been adopted. A different iterative method for solving these equations must be used depending on whether the Mach number in front of the vehicle is at or below the critical value.

Figure 4 shows the position and velocity of the vehicle within the tube as a function of time for all cases and the location of the ends of the tube. Figure 5 shows the relative Mach number and Fig. 6 the drag coefficient, drag, and momentum loss coefficient for Case 1 as the vehicle travels along the tube. The asymptotic value for the momentum loss coefficient from the long time solutions is also known. For Case 1 the relative Mach number is always below the choking value. Figures 7–9 show the velocity, entropy, and pressure both directly ahead of and behind the vehicle. The significance of the velocity and pressure is obvious, but the significance of the entropy is possibly more obscure. The changes in entropy show the effects of the irreversible friction and heat transfer processes. If these processes were not included in the calculation, then the entropy would be constant. Friction alone would only increase the entropy while heat transfer can have either effect. The fact that the entropy decreases in front of the vehicle shows that the heat transfer effect is more important than the friction and demonstrates the importance of including the heat transfer term. The

Table 1 Cases computed for far flowfield aerodynamics[a]

Case no.	Blockage ratio	Vehicle length (ft)	Vehicle friction coefficient	Closed left end (ft)	Closed right end (ft)	End of Run Vehicle travel (ft)	End of Run Duration (sec)	End of Run Final velocity (fps)
1	0.5	100	0.0025	$-\infty$	$+\infty$	280,000	1000	293
2	0.5	100	0.0025	−2000	$+\infty$	58,500	214	293
3	0.8	40	0.0025	$-\infty$	$+\infty$	229,000	800	293
4	0.8	40	0.0025	−2000	$+\infty$	229,000	800	293
5	0.8	40	0.0025	−2000	232,000	230,000	822	0

[a] Velocity for all runs: 8 fps^2 acceleration to 293 fps and constant velocity to end of run or deceleration at 8 fps^2 at end of run. Tube diameter: 10 ft. Initial tube pressure −1 atm. Vehicle starting position is $x = 0$; vehicle travels from left to right.

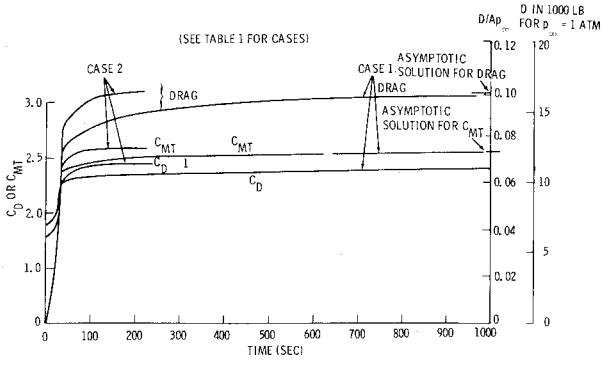

Fig. 6 Drag, drag coefficient for Cases 1 and 2.

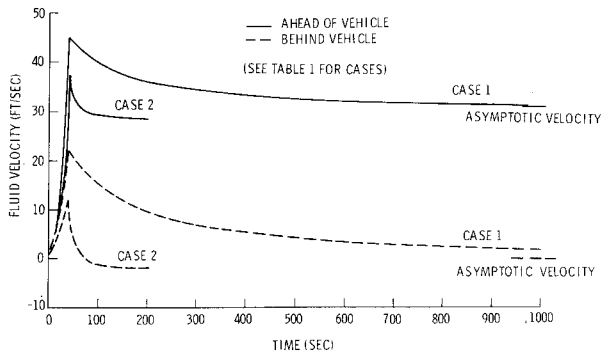

Fig. 7 Induced velocity as a function of time for Cases 1 and 2.

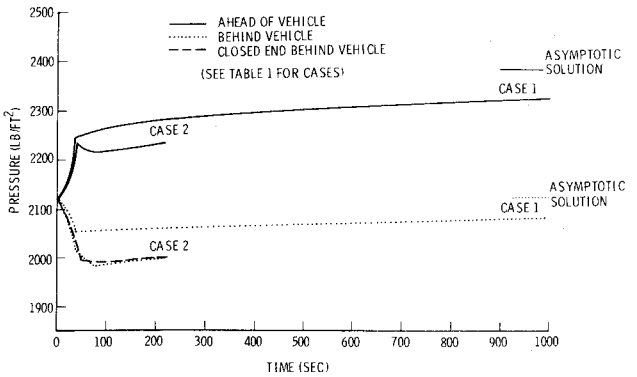

Fig. 9 Pressure as a function of time for Cases 1 and 2.

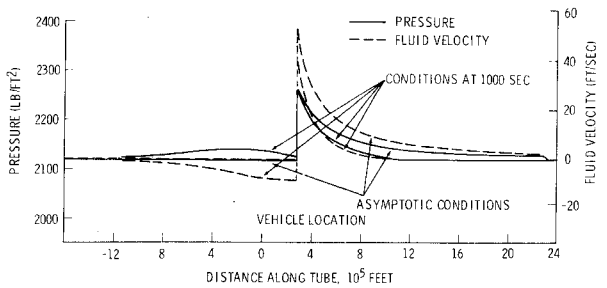

Fig. 10 Induced velocity and pressure as a function of distance along the tube at $t = 1000$ sec, Case 1 (see Table 1) and as given by the asymptotic solution.

velocity and pressure shown in Figs. 7 and 9 appear to be approaching the asymptotic limits but have not yet reached them. The asymptotic long time solution gives the rather surprising result that there is no disturbance behind the vehicle.

The velocity and pressure along the tube after the vehicle has traveled for a time of 1000 sec are shown in Fig. 10 along with the predictions of the asymptotic solutions. The condition for the asymptotic solutions to be valid is that the waves have propagated a sufficient distance so that they have been attenuated by friction and heat transfer and have become of negligible strength. The frictional compression in front of the vehicle should not have a distinct front but be asymptotic to the undisturbed conditions at infinity. Figure 10 shows that these wave fronts have not yet dissipated completely and have not propagated far enough ahead to establish the asymptotic solutions. Behind the vehicle, the conditions are also considerably different. The disturbance introduced by the passage of the train has not yet had time to attenuate to the asymptotic solution. The calculations have not been carried out to larger values of time because of the time and cost of doing so and because the tube lengths involved are considerably beyond those considered to be of practical interest.

Figures 4, 5, 11, and 12 show similar results for the large blockage ratio configuration. In this case, the magnitude of the far flowfield disturbance is much larger; the induced velocity in front of the vehicle is greater than half the velocity of the vehicle itself. The relative Mach number reaches the choking value during the acceleration of the vehicle and is constant after that. Because of the greater strength of the waves created by this vehicle, they do not attenuate to as small a value as those caused by the lower blockage ratio vehicle. Conditions do not approach as near to those given by the asymptotic solution in the time available. The velocity behind the vehicle has actually somewhat overshot the asymptotic value and gone negative.

Cases 1 and 3 were selected to assess the aerodynamic effects of both a high and low blockage ratio vehicle starting and traveling through a tube which is long enough so that there is no effect from the ends of the tube within the region affected by the vehicle. The blockage ratios were selected so that choking

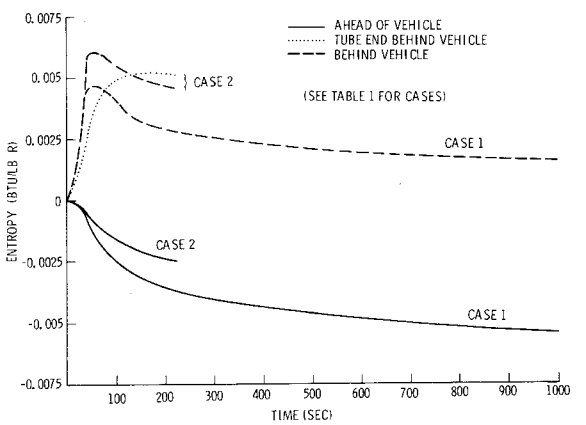

Fig. 8 Entropy as a function of time for Cases 1 and 2.

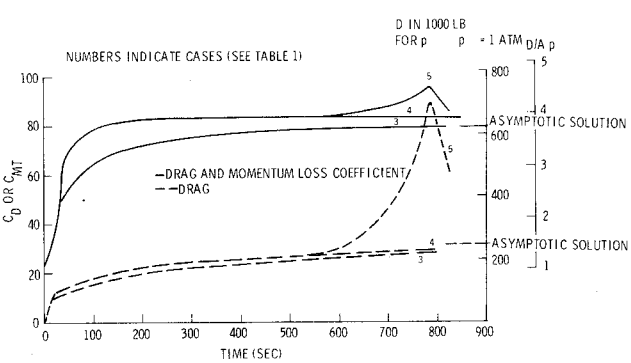

Fig. 11 Drag, drag coefficient, and momentum loss coefficient as a function of time for Cases 3–5.

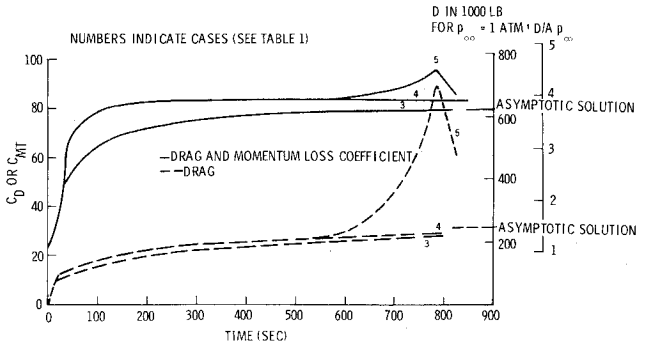

Fig. 12 Induced velocity as a function of time for Cases 3–5.

would not occur for the low blockage ratio vehicle and would occur for the high blockage ratio vehicle. The results presented here for the choked and unchoked flow configurations should be characteristic of these configurations, but calculations of a greater number of cases would be needed to confirm this expectation. The first and most obvious conclusion is that the high blockage ratio vehicle causes a much larger far flowfield effect than the low blockage ratio vehicle. As the blockage ratio and momentum loss coefficient of the vehicle decrease, the far flowfield effects are decreased and for sufficiently low blockage ratio the momentum loss coefficient and drag are too small to cause a far flowfield. Previous results[1-2] have shown that two simple solutions could be obtained to the far flowfield problem which were applicable soon after the start of vehicle travel and after a long time of vehicle travel at constant speed in a long tube. For high blockage ratio vehicles, the drag force on the vehicle is considerably larger for the long time solution than for the short time solution. One of the purposes of Cases 1 and 3 is to determine how long a distance of vehicle travel and how long a tube is required to approach these long time solutions. It is important to determined whether this is likely to occur in tube lengths of practical interest since the flowfield will then become steady and additional unsteady flow calculations will not have to be made for longer tube lengths, and to use the asymptotic long time solutions as check cases against which to validate the numerical calculations.

Case 2 and 4 are similar to 1 and 3 except that a closed end has been placed behind the starting position of the veicle at a distance of 2000 ft. The results for these cases are also shown in Figs. 5–12. This closed end causes a reduction in the velocity and pressure behind the vehicle. Both the drag coefficient, the drag of the vehicle and momentum loss coefficient are increased. However, the increase in drag is much larger for the choked vehicle. Another obvious difference between the choked and unchoked vehicle is that the closed tube end placed behind the choked vehicle has no effect on the flow in front of the vehicle which is exactly the same as it was for the previous case in which there was no closed end behind the vehicle. The increased drag is caused by the lower pressure behind the vehicle.

Case 5 is similar to Case 4 except that a closed end has been placed in the tube at 232,000 ft from the vehicle starting point. The vehicle is decelerated to stop 2000 ft from the end of the tube giving a vehicle travel of 230,000 ft or 43.6 miles. The solution is identical to Case 4 up to 215 sec when the waves first reach the far end of the tube. However, these waves must be reflected and travel back to the vehicle before there can be any change in conditions at the vehicle. These first waves are relatively weak having been attenuated by their travel through the tube and it is not until about 500 sec when the vehicle has traveled for 140,000 ft that conditions on the front of the vehicle begin to change noticeably from the previous case. However, as the vehicle continues to approach the end of the tube, the pressure between the vehicle and the end of the tube rises rapidly as well as the vehicle drag coefficient, drag, and momentum loss coefficient. The fluid which has been pushed ahead of the vehicle as it traveled down the tube is now trapped between the vehicle and the tube end and must escape around the vehicle. There is still a high pressure in front of the vehicle even after it has come to a stop. The fluid in front of the vehicle is now flowing towards the vehicle and around it to escape to the low pressure regions behind the train. The pressure is still large enough even at the time the vehicle has stopped so that the flow about the vehicle is still choked and the relative Mach number is still at the critical value.

Conclusions

1) If the flow about a vehicle is choked, changes behind the vehicle do not influence conditions in front of the vehicle and a qualitatively different flowfield from the unchoked condition is created.

2) The locations of the ends of the tube have a pronounced influence on the flowfield conditions within the tube. This effect is most pronounced for high blockage vehicles which cause a strong far flowfield.

3) When the vehicle is approaching a closed tube end located in front of the vehicle the flowfield effects are more pronounced than when it is leaving a closed tube end located behind the vehicle.

4) The distance of vehicle travel required to reach the steady state asymptotic conditions are in excess of $2(10^4)$ tube diameters (45 miles in a 10 ft diameter tube) for the cases calculated. Since the flow mechanisms and the relative importance of the viscous and inviscid terms is continuously changing as the vehicle travels along the tube, calculations and experiments in short tubes are not adequate to determine flow conditions in long tubes.

5) The analytic, long time, asymptotic flow solutions[1-2] provides an upper limit of the drag for the cases calculated. The actual vehicle drag has approached to within 10% of this value for a distance of vehicle travel of 55 miles for the low blockage vehicle of Case 1 and for a distance of vehicle travel of 43.5 miles for the higher blockage vehicle of Case 4. The relative Mach numbers and drag coefficients approach their asymptotic values more quickly but the pressure and vehicle drag lags behind.

6) The time and distance of vehicle travel required to approach the steady asymptotic values increases with vehicle blockage ratio. This result was predicted in Refs. 1 and 2 and is born out by two cases presented in this calculation.

7) The viscous effects become increasingly more important as the distance of vehicle travel increases and do not reach their full magnitude until the conditions approach their asymptotic values.

References

[1] Hammitt, A. G., "Aerodynamic Analysis of Tube Vehicle Systems," *AIAA Journal*, Vol. 10, March 1972, pp. 282–290.

[2] Hammitt, A. G., *The Aerodynamics of High Speed Ground Transportation*, Western Periodicals Co., North Hollywood, Calif., 1973.

[3] Hoppe, R. G. and Gouse, S. W., Jr., "Fluid Dynamic Drag on Vehicles Traveling Through Tubes," PB 188 451, Department of Transportation, Aug. 1969, Washington, D.C.

[4] Magnus, D. E. and Panunzio, S., "Analysis of the Near Flowfield for High Speed Vehicles in Tubes," AIAA Paper 70-140, New York, 1970.

[5] Dayman, B. and Kurtz, D. W., "Experimental Studies Relating to the Aerodynamics of Trains Traveling in Tunnels at Low Speeds," *Proceeding of the International Symposium on the Aerodynamics and Ventilation of Vehicle Tunnels*, BHRA Fluid Engineering, Cranfield, Bedford, England, 1973.

[6] Shapiro, A. H., "Compressible Fluid Flow," The Ronald Press Co., New York, 1954, pp. 907–1033.

[7] Brown, F. T., Knebel, G., and Margolis, D., "Unsteady Flow in Tubes and Tunnels," PB 204 584, Aug. 1971, Department of Transportation, Washington, D.C.